arXiv:hep-th/9506051v1 8 Jun 1995

Anomalous Supersymmetry Breaking by Instantons

A. Casher[*], V. Elkonin[†] and Y. Shamir[‡§]

School of Physics and Astronomy

Beverly and Raymond Sackler Faculty of Exact Sciences

Tel-Aviv University, Ramat Aviv 69978, ISRAEL

ABSTRACT

We show that instantons violate a supersymmetric identity in a classically supersymmetric Higgs model with no massless fermions. This anomalous breaking arises because the correct perturbative expansion in the instanton sector is not supersymmetric. The attempt to construct a manifestly supersymmetric expansion generates infra-red divergences.

1. Introduction

Asymptotically free supersymmetric gauge theories may play an important role at very short distance scales. Present day understanding of the physical properties of these theories [1-6] relies in a crucial way on the *conjecture* that non-perturbative effects do not break supersymmetry (SUSY) explicitly. The plausibility of this conjecture has been discussed in the literature. On the other hand, there are also arguments against it [7, 8].

In this paper we show that the one instanton contribution to a certain condensate violates the relevant supersymmetric identity. We consider a SUSY-Higgs model, which allows for a fully controlled calculation of non-perturbative effects. The model contains no massless fermions. Hence, the option of spontaneous "dynamical" SUSY breaking is ruled out.

Anomalous SUSY breaking is closely related to the Higgs mechanism, which provides a physical infra-red cutoff through the generation of masses. Physical observables receive non-supersymmetric contributions which arise from the non-constancy of the Higgs field in the instanton sector.

A *formally* supersymmetric expansion can be constructed in the instanton sector if the effects of the classical Higgs field, in particular the generation of masses, are incorporated *perturbatively*. Only the background gauge field is taken into account at tree level. In this formal expansion one should find supersymmetric results *provided the results are finite.*

The price paid for the perturbative treatment of mass terms is the appearance of infra-red (IR) divergences. In the literature on supersymmetric QCD there are several leading order instanton calculations with a non-vanishing scalar VEV [3, 5]. In all of them, IR divergences will arise at the next-to-leading order. In the case of the condensate calculated below, there are IR divergences already at the leading order. Moreover, the IR divergences become more and more severe as the order increases.

The anomalous breaking of SUSY is triggered by these IR divergences. While the supersymmetric calculus is valid for some (but not all) leading order calculations, the supersymmetric Feynman rules are in general ill-defined. As a result, an IR cutoff must be introduced explicitly. But the IR cutoff necessarily breaks SUSY if we are interested in the one instanton sector[1]. This sets the stage for an anomaly of a new kind. As we discuss in detail below, the IR divergences are eliminated by

---

[1] We comment that periodic boundary conditions or the compactification of R^4 to S^4 are both incompatible with the asymptotic behaviour of the Higgs field, which reflects the topology of the instanton sector.

a resummation procedure that reconstructs massive propagators from massless ones. This resummation gives rise in general to non-supersymmetric results, because the spectrum of massive modes in the instanton sector is not supersymmetric.

Let us describe the massless supersymmetric expansion in more detail. As the background gauge field one takes the pure instanton expression. (The source current in the gauge field's equation of motion is neglected to leading order). For simplicity we will henceforth assume that all masses arise through the Higgs mechanism. Mass insertions are treated perturbatively. Thus, zero modes and propagators are obtained by solving the massless field equations in the pure instanton background. The classical Higgs field itself is a solution of the equation $D^2\phi = 0$, which satisfies the boundary condition $\phi(x) \to v$ at infinity. In this framework, supersymmetric relations exist at two levels. As shown in ref. [5] the classical fields and the fermionic zero modes are related via SUSY transformations. Also, supersymmetric relations exist between the propagators, because the continuous spectrum in the pure instanton background is universal [9].

The supersymmetric expansion reflects an approximation which is valid in the instanton's core. In a Higgs model, the leading order effective action in the instanton sector is [9]

$$S_E(\rho) = 8\pi^2/g^2(\rho) + 4\pi^2 v^2 \rho^2 \,. \tag{1}$$

Here ρ is the instanton's size. The numerical coefficient of the second term, which represents the contribution of the Higgs field(s), is valid for an SU(2) gauge group [3].

Eq. (1) implies that the saddle point of the ρ-integration occurs at $\rho \sim v^{-1}$. In units of the Higgs VEV, the gauge field's strength in the core is $O(1/g)$. In contrast, the magnitude of the Higgs field is O(1), namely it is comparable to a typical quantum fluctuation on the same scale. This provides a formal justification for keeping only the gauge field at tree level. Propagators, insertions of the classical Higgs field and the full set of zero modes of the pure instanton background are all treated as elements for the construction of Feynman graphs.

The IR divergences arise from multiple mass insertions on a given line in a Feynman graph. Their physical origin is easily understood. Consider the linearized field equations taking into account *all* classical fields in the usual way. These differential equations determine the exact form of propagators and zero modes. In the core, the equations are dominated by the covariant derivative terms. Consequently, the supersymmetric expressions provide good first approximations for the exact ones.

In the transition region $v^{-1} \ll |x| \ll m^{-1}$ the equations are dominated by the free kinetic term. (Here m stands for a generic Higgs-induced mass). However, for $|x| \sim m^{-1}$ and at larger distances, the mass terms are comparable to the kinetic

3

term. At any distance scale which is large compared to the instanton's size, the massless field equations give rise to a power law behaviour. But since the relevant fields are *massive* the correct asymptotic behaviour is a falling exponential. Within the supersymmetric Feynman rules, one must sum over an arbitrary number of mass insertions on every line in order to reproduce the falling exponential. The sum of a finite number of mass insertions will in general be IR divergent.

The IR divergences of the massless supersymmetric expansion are therefore spurious, in the sense that they arise from using expressions that do not have the correct asymptotic behaviour. This statement applies to all elements of the perturbative expansion, namely, to propagators, to zero modes and to the deviations of the classical fields themselves from their limiting values.

The massive Feynman rules in the instanton sector are obtained by applying the standard variational principle. To make contact with the massless supersymmetric expansion, it is convenient to separate out the integration over the instanton's size. This is done by first fixing the size by introducing a constraint [10]. For any value of the constraint parameter one sets up a perturbative expansion in a standard manner. In the end, one integrates over the instanton's size which is now represented by the constraint parameter ρ. A judicious choice of the constraint will modify mainly the classical gauge field's equation. Physically, the source current arising from the matter part of the lagrangian tends to shrink the instanton's size, and this effect is balanced by the contribution of the constraint.

The classical fields obtained via this procedure tend exponentially to their vacuum values at large distances. The exponential asymptotic behaviour also characterizes the massive propagators and the surviving exact zero modes. As in scattering theory, this allows the removal of the finite volume cutoff, and one can work directly in the infinite volume limit.

The massive Feynman rules feature a supersymmetric set of vertices, because the classical lagrangian is supersymmetric. But in general there are no supersymmetric relations between the classical fields and the zero modes' wave functions[2]. Moreover, the massive fluctuations spectrum is no longer supersymmetric (except approximately

---

[2] Models with $N_f = 1$ are a special case. An example is the simpler Higgs model obtained by dropping the "lepton" families from the model of Sect. 2. In this case, supersymmetric relations between the classical fields and the zero modes survive to some extent also within the massive Feynman rules. This is a reminiscent of the situation in less than four dimensions, where the topologically non-trivial objects are exact solutions of the classical field equations. In both cases the SUSY violation arises from the absence of local supersymmetric relations betweens the spectra of bosonic and fermionic fluctuations. As a result, however, there are no SUSY violations at the level of tree diagrams. See ref. [7] for more details.

at very short distances). The linearized bosonic field equation and the square of the Dirac operator define two Schrödinger-like operators. Due to the non-constancy of the Higgs field in the instanton's core, these Schrödinger operators involve *different* potentials. Consequently, massive bosonic and fermionic eigenstates are not related by the action of a local differential operator [7]. Therefore, the breaking of SUSY is ultimately attributed to the non-invariance of the path integral measure.

We summarize the relation between the massive Feynman rules and the massless ones by considering the example of an exact zero mode, i.e. a zero mode that survives the introduction of the Higgs field. Other elements of the Feynman rules (propagators etc.) exhibit analogous behaviour. The l.h.s. of any field equation can be written as $H_0 + V$, where V contains the dependence on the Higgs field and H_0 contains all the rest. Let Ψ_0 be a zero mode of H_0 and Ψ the corresponding zero mode of $H_0 + V$. Formally, V is small compared to H_0, and so we may think of reexpanding Ψ using the Born series $\Psi = \Psi_0 - G_0 V \Psi_0 + \cdots$. But in general this is not possible because V contains a mass term that changes the asymptotic behaviour. Individual terms in the Born series have divergent norms, and their insertion in a Feynman graph gives rise to IR divergences.

In practice, one has to distinguish between two cases. Suppose that the massless Feynman rules give rise to a finite answer for some observable (or, more generally, for some sub-diagram) at the leading order. As far as a given zero mode is concerned, this will typically happen when the leading order result involves only the "zeroth approximation" Ψ_0 which is obviously normalizable. Notice that the difference $\Psi - \Psi_0$ is normalizable too. Replacing Ψ_0 by $\Psi - \Psi_0$ will measure the difference between the correct result and the (still finite) prediction of the massless expansion. One can show that, up to logarithmic corrections, the contribution of the difference $\Psi - \Psi_0$ will be damped by two powers of the coupling constant(s). A similar pattern is found for other elements of the Feynman graphs. In conclusion, if the massless supersymmetric rules give rise to a finite answer for a (sub-)graph at the leading order, then the answer is valid at that order, and it will be reproduced by the massive Feynman rules.

Whenever the massless supersymmetric rules give rise to IR-divergent expressions, the massive Feynman rules must be invoked. The mass terms then provide a *physical* cutoff for the formally IR-divergent integrals. Below we encounter a sub-graph which is equal, within the massless supersymmetric rules, to the norm squared of the first Born correction $\Psi_1 = -G_0 V \Psi_0$ to a certain zero mode. However, the norm of Ψ_1 is IR-divergent.

Physically, Ψ_1 represents a new field component that the original zero mode develops due to the mass terms. Using the massive Feynman rules, what has to be

calculated is the norm of the new component. (The overall normalization of the zero mode is still determined by the original component). The new component's norm has a leading logarithmic piece which is easily computed, and which contributes to the final result eq. (6).

The IR divergences signal the onset of a *non-analytic* dependence on Higgs masses, and, hence, on coupling constants. The condensate calculated below features a non-analytic dependence on two Yukawa couplings. This result is of course beyond the scope of the massless supersymmetric expansion, which contains only positive powers of the Yukawa couplings. More generally, we expect the appearance of analogous non-analytic dependence on the *gauge coupling* too. Technically, disentangling non-analytic short distance effects (the RG flow) from long distances ones is more complicated in this case.

This paper is organized as follows. In Sect. 2 we define the SUSY-Higgs model. In Sect. 3 we present our results. Sect. 4 contains our conclusions. Some technical detail are relegated to an Appendix.

2. The model

The charged fields of our SU(2)-Higgs model are the same as in supersymmetric QCD with $N_c = N_f = 2$. Two charged doublets play the role of Higgs superfields. The other pair of charged superfields together with a pair of neutral ones make two supersymmetric "lepton" families. The Higgs superpotential is

$$W_1 = h\Phi_0 \left(\frac{1}{2}\epsilon_{ij}\epsilon_{AB}\,\Phi_{iA}\Phi_{jB} - v^2 \right) . \tag{2}$$

Here $\Phi_0 = (\phi_0, \psi_0)$ is a neutral chiral superfield. $\Phi_{iA} = (\phi_{iA}, \psi_{iA})$ contain the two Higgs doublets and their fermionic partners. The indices $A, i = 1, 2$ correspond to SU(2) colour and flavour groups respectively. (The flavour SU(2) plays the role of SU(2)$_R$ in the analogy to the supersymmetric Standard Model). We use the following representations $T^a_{AB} = -\frac{1}{2}\sigma^a_{BA}$ and $F^a_{ij} = \frac{1}{2}\sigma^a_{ij}$ for the colour and flavour generators respectively.

The two extra charged superfield are denoted $\eta_{A\pm}$, and the two extra neutral ones are $\xi_{i\pm}$. These letters will also be used to denote the fermionic components. The scalar components are denoted $\tilde{\eta}_{A\pm}$ and $\tilde{\xi}_{i\pm}$. The $\pm$ index labels the two "lepton" families. Notice that these families form a doublet under a horizontal SU(2). The full superpotential is

$$W = W_1 + W_2 , \tag{3}$$

where

$$W_2 = y\,\epsilon_{ij}\epsilon_{AB}\,\Phi_{jB}\left(\xi_{i+}\,\eta_{A-} - \xi_{i-}\,\eta_{A+}\right)$$
$$+ m_0\,\epsilon_{ij}\,\xi_{i+}\xi_{j-}\,. \tag{4}$$

The mass parameter m_0 will be treated as a small perturbation[3] and we will work to first order in m_0.

The classical potential has a unique supersymmetric minimum (up to colour and flavour transformations). The only non-vanishing VEV is $\langle\phi_{iA}\rangle = v\delta_{iA}$. This minimum breaks the gauge symmetry completely, but it leaves unbroken the diagonal SU(2) generated by $T^a + F^a$. Under this vector SU(2), the two Higgs superfields decompose into a singlet $\Phi' = \delta_{iA}\Phi_{iA}/\sqrt{2}$ and a triplet $\Phi^a = \sigma_{iA}^a\Phi_{iA}/\sqrt{2}$.

All fields acquire masses through the Higgs mechanism. In the triplet sector (which includes the gauge and the Φ^a supermultiplets) the mass is $\mu = gv$. The mass of the singlet fields Φ' and Φ_0 is $m = \sqrt{2}hv$. For $m_0 = 0$, the mass of the lepton families is $m_1 = yv$.

The model has two approximate R-symmetries. U(1)$_R$ is a non-anomalous symmetry, which becomes exact in the limit $m_0 = 0$. The other one, denoted U(1)$_X$, is a classical symmetry of the full lagrangian, but it is broken explicitly by instantons. The fermion charges under the R-symmetries are given in Table 1 in units of the gaugino's charge. As usual, the charges of the corresponding scalars are related by $Q_R(scalar) = Q_R(fermion) + 1$.

	ψ_{iA}	ψ_0	$\eta_{A\pm}$	$\xi_{i\pm}$
U(1)$_R$	-1	1	-1	1
U(1)$_X$	-1	1	0	0

Table 1: Fermion charges under the R-symmetries

---

[3] The perturbative treatment of m_0 does not generate any IR divergences because all the fields are already massive for $m_0 = 0$. Our results can also be regarded as a calculation of the integrated form of the r.h.s. of eq. (5) in the model with $m_0 = 0$.

3. Results

3.1 The SUSY identity

Let $\mathcal{O}(x)$ denote the lowest component of a gauge invariant chiral superfield and let $\bar{Q}$ be a SUSY generator. Using $[\bar{Q}, \mathcal{O}(x)] = 0$ one arrives at the following on-shell SUSY identity

$$
\begin{aligned}
0 &= \left\langle \mathcal{O}(z) \{ \bar{Q}, \tilde{\xi}_{i+}^* \bar{\xi}_{j-}(x) \} \right\rangle \\
&= \left\langle \mathcal{O}(z) \left((1/2) \, \bar{\xi}_{i+} \bar{\xi}_{j-}(x) + y\epsilon_{jk}\epsilon_{AB} \, \tilde{\xi}_{i+}^* \phi_{kA} \tilde{\eta}_{B+}(x) \right) \right\rangle .
\end{aligned}
\tag{5}
$$

This identity is related to the analytic properties of the condensate $\langle \mathcal{O} \rangle = \langle \mathcal{O}(z) \rangle$ as follows. Let us assume that m_0 in eq. (4) is a complex parameter. On the second row of eq. (5) we contract with ϵ_{ij} and integrate over x. A similar identity is obtained by the interchange of $\xi_+ \leftrightarrow \xi_-$ and $\eta_+ \leftrightarrow -\eta_-$. Taking into account the two identities we arrive at the variation of $\langle \mathcal{O} \rangle$ with respect to m_0^*. Therefore, eq. (5) requires that $\langle \mathcal{O} \rangle$ be a function of m_0 only, but not of m_0^* [4].

3.2 Calculation of $\langle \phi_0 \rangle$

Our main result is that the SUSY identity eq. (5) is violated for $\mathcal{O} = \phi_0$. An explicit calculation gives rise to

$$
\langle \phi_0 \rangle = m_0^* \frac{\Lambda^4}{v^4} \frac{y^2}{4\pi^2 g^4 h} \log y + \cdots .
\tag{6}
$$

The dots stand for subleading terms[4]. Λ is the one-loop RG invariant scale of the theory. We expect similar violations for other condensates, such as for example $\langle \lambda\lambda \rangle$. However, for reasons that we explain below the calculation of the m_0^*-dependence of $\langle \lambda\lambda \rangle$ is more complicated.

In the calculation of $\langle \phi_0 \rangle$ we adopt the following strategy. Diagrams will first be drawn using the massless supersymmetric rules, and we will try to apply these rules to evaluate every sub-graph. In view of the relation between the massive Feynman rules and the massless ones, as discussed in the introduction, the result for a given sub-graph is valid *as long as it is finite*. When the massless rules produce IR divergent expressions, the massive Feynman rules will be invoked to calculate the relevant integrals.

The diagrams that contribute to the leading order result eq. (6) are depicted in Figs. 1 and 2. The two diagrams correspond to the two terms on the last row of

---

[4] The anti-instanton sector makes a contribution to $\langle \phi_0^* \rangle$ that satisfies the on-shell relation $\langle \phi_0^* \rangle = \langle \phi_0 \rangle^*$. We comment that $\langle \phi_0 \rangle$ vanishes to all orders in perturbation theory because ϕ_0 carries a non-zero $\mathrm{U}(1)_X$ charge.

eq. (5). The vertex marked with a thick cross is linear in m_0^*. The dotted lines that end with a cross represent insertions of the classical Higgs field. They differ from ordinary mass insertions by the presence of short range potential terms that arise from the non-constancy of the Higgs field in the instanton's core.

Each thick line that emanates from the instanton (the shaded circle) represents one of the eight zero modes that the model had had in the absence of the Higgs field. These include the four gaugino zero modes and one zero mode for each charged doublet. With the classical Higgs field turned on, only the λ^{SS} pair and the $\eta_\pm$ pair remain exact zero modes (with modified wave functions that contain new field components). The Higgsino and λ^{SC} zero modes mix through the Higgs field. However, they are still *approximate* zero modes because the Higgs field is a small perturbation over their support. More precisely, the λ^{SC} and Higgsino zero modes become either resonances or bound states with non-zero eigenvalues. (The former possibility is more likely). This is the physical justification for treating their mixing using the massless Feynman rules, with the usual reservation that this does not give rise to IR divergences. Further details on both the exact and the approximate zero modes are given in the Appendix.

Before we continue with the calculation of Figs. 1 and 2 let us discuss the role of other diagrams. If we only count powers of coupling constants that come from the vertices and ignore the IR divergences momentarily, we should consider diagrams which are $O(g^4 y^2 h)$. Now, within the massless Feynman rules, all these diagrams have in common a quadratic IR divergence due to the external ϕ_0 leg. If we try to use a (free) massless propagator instead of the correct ϕ_0 propagator, we encounter at some point an integral of the form $\int d^4x/x^2$. As we discuss below, within the massive Feynman rules the quadratic divergence boils down to a factor of $1/m^2$. We then use $m^2 = 2h^2 v^2$ to separate out a dimensionful factor of v^2. The remaining $1/h^2$, together with the explicit factor of h coming from the vertex, gives rise to the $1/h$ factor in eq. (6).

Apart from the common quadratic IR divergence, there are several diagrams that contain an extra logarithmic IR divergence of the form $\int d^4x/(x^2+\rho^2)^2$. The physical IR cutoff of such an integral is an inverse mass scale. Thus, the integral behaves like the logarithm of the relevant Higgs induced mass times ρ. In view of the relation $\rho \sim v^{-1}$, this is equivalent to the logarithm of a coupling constant.

An enhancement factor of $\log y$ arises if and only if the logarithmic divergence comes from the "lepton" sector, the relevant diagrams being Figs. 1 and 2. As our explicit calculation shows, the leading logs do not cancel between the two diagrams, which sum up to the final result eq. (6).

Notice that we have indicated in the figures which insertion of the Higgs field corresponds to ϕ_{iA} and which to its complex conjugate. Other diagrams that are formally of the same order can be obtained by replacing one insertion of the Higgs field and one insertion of its complex conjugate by a $\langle \phi \phi^* \rangle$ propagator. However, the resulting diagrams no longer have the extra logarithmic divergence, because the propagators provide extra powers of $1/x^2$ (some examples are discussed in part III of the Appendix). The leading logs arise only from diagrams with a maximal number of insertions of the Higgs field.

Within the massless Feynman rules, there are also individual diagrams containing logarithmic IR divergences related to the λ^{SC} and Higgsino zero modes. But now the offensive $1/(x^2 + \rho^2)^2$ behaviour cancels out between different diagrams *before* the ρ integration. This implies that the corresponding diagrams of the *massive* Feynman rules contain no logarithmic factors[5]. The physical reason for this behaviour is the following. A slow $1/x^2$ decrease of a zero mode's wave function at intermediate distances can arise only from new field components not present in the original zero mode. The new subleading field components are well defined in the case of an *exact* zero mode. But subleading field components of *approximate* zero modes cannot be disentangled from the continuous spectrum. For further details see part III of the Appendix.

We now return to the derivation of eq. (6). The diagrams are evaluated with the measure (see e.g. ref. [4])

$$2^9 \pi^6 \Lambda^4 g^{-8} \int d\rho^2 \rho^2 e^{-4\pi^2 v^2 \rho^2} \ldots \tag{7}$$

For Fig. 1 the integrand of the ρ-integral is

$$\left(\frac{g^2 v^2}{2} \right) \left(\frac{g^2 \rho^2}{8h} \right) \left(m_0^* (yv\rho)^2 \log y \right) . \tag{8}$$

Let us explain this expression. Consider first the mixing of the λ^{SC} and Higgsino zero modes [3] through the Yukawa-gauge coupling $ig\sqrt{2}\,\lambda^a \phi_A^* T_{AB}^a \psi_B$. To leading order there are no IR divergences, and one can calculate the mixing using formal first order perturbation theory. Substituting the pure instanton expressions for the zero modes eqs. (A.6) and (A.7), and for the Higgs field eqs. (A.2) and (A.4), we arrive at the first factor in eq. (8).

The second factor corresponds to the ϕ_0 tadpole, namely to the ϕ_0 line that emanates from the pair of λ^{SS} zero modes (see Fig. 3). It is convenient to trade the

---

[5] Had the logarithmic divergences coming from the gaugino-Higgsino sector *not* cancelled out, they would have represented an independent contribution to $\langle \phi_0 \rangle$, because they could not give rise to $\log y$, but only to a linear combination of $\log g$ and $\log h$.

integration over the instanton's collective coordinates with an integration over the external point z, keeping the instanton at the origin. The tadpole is

$$\frac{h}{2}\epsilon_{kl}\epsilon_{ij}\epsilon_{AB}\int d^4x\, d^4z\, \widetilde{G}(z,x)\,\bar{\psi}_{iA}^k(x)\bar{\psi}_{jB}^l(x)\,. \tag{9}$$

Here $\widetilde{G}(z,x)$ is the ϕ_0 propagator and $\bar{\psi}_{iA}^k(x)$ is a new field component of the k-th λ^{SS} zero mode $(k=1,2)$. We immediately see that the attempt to treat ϕ_0 as a massless field gives rise to a quadratic IR divergence. Within the massive Feynman rules, the ϕ_0 propagator is defined by

$$(-\Box_z + m^2 + U)\widetilde{G}(z,x) = \delta^4(z-x)\,. \tag{10}$$

The short range potential U is a function of the radial coordinate $r = |z|$ only. Explicitly $U(r) = m^2(\varphi^2(r) - 1)$. (See eq. (A.2) for the definition of $\varphi(r)$). The short range potential *can* be neglected to leading order. We therefore substitute a free massive propagator for $\widetilde{G}(z,x)$ and find

$$\int d^4z\, \widetilde{G}(z,x) = \frac{1}{m^2}\,. \tag{11}$$

Notice that the result is independent of x.

The rest of eq. (9) does not contain any divergent factors. Instead of using the exact wave function of the $\bar{\psi}(x)$ component of the λ^{SS} zero mode, we can apply first order massless perturbation theory. The general formula for the first Born correction is $\Psi_1 = -G_0 V \Psi_0$. In the present case G_0 stands for the $\left\langle \psi\bar{\psi}\right\rangle_0$ propagator in the pure instanton background, V stands for the Yukawa-gauge coupling as a function of the Higgs field, Ψ_0 stands for the original λ^{SS} zero mode eq. (A.5) and Ψ_1 stands for the new $\bar{\psi}(x)$ field component. In practice, instead of finding $\bar{\psi}(x)$ by integration, it is easier to solve the corresponding differential equation $H_0\Psi_1 = -V\Psi_0$, where H_0 is the massless covariant Dirac operator. The result is

$$\bar{\psi}_{iA\alpha}^k(x) = \frac{igv}{2\pi}\frac{\epsilon_{i\alpha}\delta_{Ak}\,\rho^2}{(x^2+\rho^2)^{\frac{3}{2}}}\,. \tag{12}$$

Here α is the spinor index. Carrying out the x-integration and using $m^2 = 2h^2v^2$ we arrive at the second factor in eq. (8).

The last factor in eq. (8) corresponds to the upper part of Fig. 1. It takes the form

$$m_0^*\,\epsilon_{ij}\int d^4x\, \bar{\xi}_{i+}(x)\bar{\xi}_{j-}(x)\,, \tag{13}$$

where $\bar{\xi}_\pm(x)$ is a new field component of the $\eta_\mp$ zero mode. As before, we try to use the first Born correction. The result is

$$\bar{\xi}_{i\alpha\pm}(x) = \mp\frac{yv}{2\pi}\frac{\epsilon_{i\alpha}\,\rho}{x^2+\rho^2}\,. \tag{14}$$

11

In this case the spacetime integration is logarithmically IR divergent. The true form of $\bar{\xi}_{\pm}(x)$ is determined by eq. (A.12). It agrees with eq. (14) for $|x| \ll m_1^{-1}$, whereas for $|x| \gg m_1^{-1}$, $\bar{\xi}_{\pm}(x)$ becomes a falling exponential. (That the transition occurs at the distance scale m_1^{-1} is a general feature of massive linear equations. See part II of the Appendix for more details).

Let us write $d^4x = r^3\, dr\, d\Omega$, and split the radial integration in eq. (13) into three regions

$$\int_0^\infty = \int_0^\rho + \int_\rho^{m_1^{-1}} + \int_{m_1^{-1}}^\infty . \tag{15}$$

The integral is dominated by the intermediate region, where one has $\bar{\xi}_+\bar{\xi}_-(x) \sim 1/x^4$, leading to

$$\int_\rho^{m_1^{-1}} \frac{d^4x}{x^4} = -2\pi^2 \log(m_1\rho) . \tag{16}$$

Notice that $\log(m_1\rho) = \log y + \log(v\rho)$, and that $\log(v\rho)$ is $O(1)$. Neglecting $O(1)$ contributions, we complete the calculation by adding the appropriate prefactors required by eq. (14). The result is the last factor in eq. (8).

The calculation of Fig. 2 is similar. Using massless perturbation theory we find the "induced scalar field"

$$\tilde{\eta}_{A\pm}^k(x) = -\frac{ig}{4\sqrt{2}\,\pi^2} \frac{\epsilon_{kl}x^\mu \bar{\sigma}_{lA}^\mu}{(x^2 + \rho^2)^{\frac{3}{2}}} . \tag{17}$$

This induced field is obtained by solving the massless field equation with a source given by the product of the k-th λ^{SC} zero mode and an η zero mode. The second induced field, whose source is the product of the n-th Higgsino zero mode ($n = 1, 2$) and the other η zero mode, is

$$\tilde{\xi}_{i\pm}^{n*}(x) = \pm \frac{y}{4\pi^2} \frac{\epsilon_{in}}{x^2 + \rho^2} . \tag{18}$$

Now we have a logarithmic IR divergence from the integral

$$m_0^*\, y\, \epsilon_{AB} \int d^4x\, \tilde{\xi}_{i\pm}^{n*}(x)\phi_{iA}(x)\tilde{\eta}_{B\pm}^k(x) . \tag{19}$$

As before, the leading log is obtained by substituting eqs. (17) and (18) in eq. (19) and imposing a physical cutoff at $r_0 \sim m_1^{-1}$. Summing the leading logs from the two diagrams we find

$$\langle \phi_0 \rangle = m_0^* \Lambda^4 v^2 \frac{16\pi^4 y^2}{g^4 h} \log y \int d\rho^2\, \rho^4 e^{-4\pi^2 v^2 \rho^2} (2\pi^2 v^2 \rho^2 - 1) . \tag{20}$$

In this equation, the first and second terms in parenthesis correspond to Figs. 1 and 2 respectively. Carrying out the ρ-integration we finally arrive at eq. (6). Further discussion of the physical mechanism underlying this result is given in Sect. 4.

3.3 Comparison of $\langle \phi_0 \rangle$ and $\langle \lambda\lambda \rangle$

In this paper we are not concerned so much with the numerical value of $\langle \phi_0 \rangle$, but with the fact that this condensate violates the SUSY indentity eq. (5). Since we are dealing with a matter of principle, it is worthwhile to give an alternative derivation of the existence of SUSY violations.

Examining the various leading order supersymmetric results found in the literature [3, 5] we observe that, typically, there are diagrams that contain a different number of insertions of the Higgs field. Each classical field provides a factor of v and, to match dimensions, the diagram must contain compensating powers of ρ. The relative weight of different diagrams is therefore ρ-dependent, and the supersymmetric result depends crucially on performing the ρ-integration.

In the calculation of $\langle \phi_0 \rangle$ the two diagrams Figs. 1 and 2 have a different ρ-dependence too. But now the ρ-integration gives rise to a SUSY violating result. Introducing to the dimensionless variable

$$s \equiv 4\pi^2 v^2 \rho^2 \,, \tag{21}$$

we can rewrite eq. (20) as

$$\langle \phi_0 \rangle = m_0^* \frac{\Lambda^4}{v^4} \frac{y^2}{4\pi^2 g^4 h} \log y \int ds\, e^{-s} s^2 (c_1 s - c_2) \,. \tag{22}$$

The numerical values of the constants are $2c_1 = c_2 = 1$. The reason why we have introduced them will be explained shortly.

Let us now discuss the m_0^*-dependence of $\langle \lambda\lambda \rangle$. The diagrams that contribute to the leading log are closely related to Figs. 1 and 2. We only have to replace the ϕ_0 tadpole (Fig. 3) by a new sub-graph in which the two λ^{SS} zero modes go directly to the external point (see Fig. 4). The other parts of the diagrams as well as the symmetry factors are unchanged. In the case of the diagram related to Fig. 1, this amounts to replacing the $g^2\rho^2/(8h)$ factor in eq. (8) by 2. The coefficient of the leading log of $\langle \lambda\lambda \rangle$ takes the form

$$\langle \lambda\lambda \rangle = m_0^* \frac{\Lambda^4}{v^2} \frac{16y^2}{g^6} \log y \int ds\, e^{-s} s (c_1 s - c_2) \,. \tag{23}$$

Notice that the expression in parenthesis is the same as in eq. (22). This expression corresponds to the parts of Figs. 1 and 2 that are unchanged in the calculation of $\langle \lambda\lambda \rangle$. A comparison of eqs. (22) and (23) reveals that the integrand of eq. (22) contains an extra power of s, i.e. an extra power of ρ^2. Consequently, regardless of the numerical values of the constants c_1 and c_2, *the leading SUSY violating logs cannot vanish simultaneously* for $\langle \phi_0 \rangle$ and $\langle \lambda\lambda \rangle$.

As we have explained above, the power of ρ^2 in every graph is determined by the discrepancy between the explicit factors of v and the dimensionality of the diagram (taking into account the common dimensionful constant $m_0^* \Lambda^4$). In the case of $\langle \lambda\lambda \rangle$, the integration over the pair of λ^{SS} zero modes gives rise to no factors of v. In the case of the ϕ_0 tadpole, there is a factor of v^2 coming from the two insertions of the Higgs field indicated explicitly in Fig. 3. But this v^2 is cancelled by a $1/v^2$ coming from the zero momentum Fourier transform of the ϕ_0 propagator: $m^{-2} = (2h^2 v^2)^{-1}$. This non-analytic dependence on v^2 arises because the massive propagator is obtained from the massless one by an infinite sum over an arbitrary number of mass insertions. The overall power of v is eventually the same in both cases. Since the dimension of $\langle \phi_0 \rangle$ is smaller than the dimension of $\langle \lambda\lambda \rangle$ by two, there has to be an extra power of ρ^2 in the case of $\langle \phi_0 \rangle$.

Substituting the numerical values of c_1 and c_2 and performing the ρ-integration, we find that the coefficient of the leading log cancels between the two terms in eq. (23). Thus, contrary to the case of $\langle \phi_0 \rangle$, there is no logarithmic enhancement for $\langle \lambda\lambda \rangle$. A calculation of the contribution with no logarithmic enhancement to $\langle \lambda\lambda \rangle$ should involve the following ingredients. First, the cancellation of logarithmic IR divergences between the two diagrams discussed above leaves behind a finite non-zero remainder. Additional contributions arise from massless diagrams in which pairs of classical fields have been replaced by propagators. These diagrams are individually finite.

All the diagrams mentioned above belong to the same order in the massless expansion. But this is not the end of the calculation. Comparable contributions arise from higher order terms in the Born series. Although diagrams with more insertions of the Higgs field are formally of higher order, they contain stronger IR divergences that compensate for the extra powers of the coupling constant y. We first observe that even terms in the Born series represent corrections to the η-component of the "lepton" zero modes, whereas odd terms are corrections to the $\bar{\xi}$-component. Denoting the $(2n-1)$-st correction by $\bar{\xi}^{(n)}(x)$ one has

$$\bar{\xi}^{(n)}(x) \sim \rho \, m_1^{2n-1} x^{2n-4} \,, \qquad \rho \ll |x| \ll m_1^{-1} \,. \tag{24}$$

In this equation we have shown only the leading power law behaviour and suppressed logarithmic factors. We see that the Born series represent an expansion in powers of $m_1 x$. But the physical cutoff of the x-integration occurs at $x \sim m_1^{-1}$. Thus, after the x-integration each extra power of x^2 leads to an extra power of $1/m_1^2$. A similar pattern is found for higher order corrections to the induced scalar fields (the subgraph in the upper-left part of Fig. 2). The final result is that the massless expansion breaks down because it becomes an expansion in $m_1^2/m_1^2 = 1$.

14

The conclusion is that, in order to calculate the leading order value of $\langle\lambda\lambda\rangle$, one must sum contributions from all orders in the massless expansion. Within the massive Feynman rules, this is equivalent to a calculation of the non-logarithmic terms that arise from the exact form of the zero modes and the induced scalar fields in the "lepton" sector. We expect that eventually $\langle\lambda\lambda\rangle$ will be non-zero because the linearized massive field equations are manifestly not supersymmetric.

4. Discussion

The definition of the path integral measure requires one to specify a complete set of quantum modes. In the vacuum sector, the free (massive or massless) field equations define the same set of plane waves for both bosons and fermions. Consequently, there are no SUSY violations in the vacuum sector.

In the instanton sector, there are *three* relevant complete sets of modes. The first complete set consists of the massless modes pertaining to the self-dual classical instanton solution. This basis is universal for all spins, and it defines the formally supersymmetric perturbative expansion. The massive field equations, that contain the Higgs field, define two more complete sets: one for the bosons and one for the fermions. The massive bosonic and fermionic modes are different from each other, as well as from the massless modes. *The path integral measure must be defined using the basis of massive modes*, because the alternative basis of massless modes leads to IR divergences.

In fact, the massless spectrum is not exactly supersymmetric. The massless perturbative expansion is well defined only in a finite box. Since there are no supersymmetric boundary conditions in the instanton sector, the result is an $O(1/R)$ discrepancy between the bosonic and fermionic spectra (R is the size of the box). The explicit $1/R$ breaking terms are multiplied by positive powers of R coming from the IR divergences, and so they can (and do) leave behind a finite effect in the infinite volume limit.

The massive fluctuations spectrum, which is the appropriate one in the infinite volume limit, is manifestly not supersymmetric. The finite discrepancy between the spectra of massive fluctuations arises because of the non-constancy of the Higgs field in the instanton's core. The crucial effect is the existence of terms that involve *derivatives* of the classical Higgs field in the Schrödinger-like operators that define the bosonic and fermionic modes. (In the case of the fermions we refer to the square of the Dirac operator). Derivatives of the Higgs field appear as potentials in these

Schrödinger operators, and one can explicitly check that the potentials are different for bosons and fermions for any choice of the Higgs field.

Let us now reexamine the SUSY violating result found in Sect. 3. The existence of different powers of ρ in the final expressions eqs. (22) and (23) means that the saddle point of the ρ-integration is different in each diagram. In other words, the effective value of ρ depends on the operator that we measure. This is not surprising. The integration over ρ is gaussian, and so ρ really represents a quantum mode.

The logarithmic terms arise from the product of two wave functions that behave like $1/x^2$ in the intermediate region. They depend on the effective value of ρ in two ways. The most important effect is that the normalization of the relevant wave functions is ρ-dependent. A secondary effect is that the short distance cutoff of the $1/x^2$ behaviour is determined by ρ. In the intermediate region, the equations of motion are locally supersymmetric to a first approximation. The SUSY violation arises because one cannot solve the equations with supersymmetric boundary conditions both a the origin and at infinity. Physically, the asymptotic region is supersymmetric because it is a free vacuum. The breaking of SUSY originates from the Higgs dependent part of instanton's core. In the calculation, it takes the form of non-supersymmetric values for the effective ρ.

The Higgs model and the observables discussed in this paper were chosen for reasons of technical convenience. In essence, the anomalous breaking of SUSY was shown to be directly related to the IR divergences of massless perturbation theory. We thus conjecture that the SUSY anomaly is a generic property of asymptotically free supersymmetric gauge theories.

Specifically, we proved the failure of the holomorphicity of physical observables constructed from the lowest components of gauge invariant chiral superfield. The conventional treatment of supersymmetric QCD depends heavily on the assumed holomorphicity, leading to conclusions such as the existence of a pathological runaway behaviour. We believe that these conclusions have to be reexamined in view of the failure of holomorphicity found in this paper.

16

Appendix

I. Zero modes in the pure instanton background

In the instanton sector, the classical gauge field is given by

$$A_\mu^a = \frac{2}{g} \frac{\bar\eta_{a\mu\nu} x^\mu}{r} a(r) , \tag{A.1}$$

and the classical Higgs field is

$$\phi_{iA} = iv \frac{\bar\sigma_{iA}^\mu x^\mu}{r} \varphi(r) . \tag{A.2}$$

We have suppressed the collective coordinate x_0^μ. For $mr \ll 1$ one has

$$a(r) = r/(r^2 + \rho^2) , \tag{A.3}$$

$$\varphi(r) = r/(r^2 + \rho^2)^{\frac{1}{2}} . \tag{A.4}$$

For $mr \gg 1$ these expressions are no longer valid. Both the gauge field and the Higgs field tend exponentially to their limiting values $a(r) \to 1/r$ and $\varphi(r) \to 1$. In this paper we only need the explicit form of the classical fields for $mr \ll 1$.

We next turn to the fermionic zero modes. The measure eq. (7) requires the normalization $\int d^4x |\Psi|^2 = 1$ for all zero modes. In the pure instanton background the normalized gaugino zero modes are[6]

$$(\lambda_\alpha^a)_k^{SS} = \frac{\sqrt{2}\,\rho^2}{\pi} \frac{\sigma_{\alpha k}^a}{(x^2 + \rho^2)^2} , \tag{A.5}$$

$$(\lambda_\alpha^a)_k^{SC} = \frac{\rho}{\pi} \frac{\sigma_{\alpha l}^a x^\mu \sigma_{lk}^\mu}{(x^2 + \rho^2)^2} , \tag{A.6}$$

where $k = 1, 2$. The zero modes of the four charged doublets are identical except for the flavour quantum numbers. The Higgsino zero modes are

$$(\psi_{iA\alpha})_n = \frac{\rho}{\pi} \frac{\delta_{in}\delta_{A\alpha}}{(x^2 + \rho^2)^{\frac{3}{2}}} , \tag{A.7}$$

where $n = 1, 2$. The "lepton" zero modess are

$$\eta_{A\alpha\pm} = \frac{\rho}{\pi} \frac{\delta_{A\alpha}}{(x^2 + \rho^2)^{\frac{3}{2}}} . \tag{A.8}$$

---

[6] The euclidean partition function of supersymmetric theories is defined using a Majorana representation for the fermions. Consistency of this representation determines the global phase of the zero modes' wave functions. The Majorana representation is mandatory for the gaugino but it is convenient to treat the matter fermions analogously. See e.g. ref. [7] for more details.

II. Exact zero modes

When we turn on the Higgs field, the λ^{SS} and the $\eta_\pm$ pairs remain exact zero mode, but with new field component and modified wave functions. The λ^{SS} pair now takes the form [3]

$$(\lambda_\alpha^a)_k = \sigma_{\alpha k}^a \hat{f} \tag{A.9a}$$

$$(\bar{\psi}_{iA\alpha})_k = i\epsilon_{i\alpha}\delta_{Ak}\hat{g} + i\epsilon_{\beta\alpha}x^\mu x^\nu \sigma_{Ai}^\mu \bar{\sigma}_{\beta k}^\nu \hat{h} \tag{A.9b}$$

$$(\psi_{0\alpha})_k = i\delta_{\alpha k}\hat{p} \tag{A.9c}$$

The hat denotes radial functions. The "lepton" zero modes are now given by

$$\eta_{A\alpha\pm} = \delta_{\alpha A}\hat{u} \tag{A.10a}$$

$$\bar{\xi}_{i\alpha\mp} = \pm\epsilon_{i\alpha}\hat{w} \tag{A.10b}$$

The quantum numbers of the different field components of these zero modes can be found in Table 2. The conserved angular momenta in the instanton sector are

$$K_1^a = S_1^a + L_1^a + T^a,$$
$$K_2^a = S_2^a + L_2^a + F^a. \tag{A.11}$$

channel	S_1	S_2	T	F	L	K_1	K_2
λ^a	$\frac{1}{2}$	0	1	0	0	$\frac{1}{2}$	0
$\bar{\psi}_{iA}$	0	$\frac{1}{2}$	$\frac{1}{2}$	$\frac{1}{2}$	0,1	$\frac{1}{2}$	0
ψ_0	$\frac{1}{2}$	0	0	0	0	$\frac{1}{2}$	0
η_A	$\frac{1}{2}$	0	$\frac{1}{2}$	0	0	0	0
$\bar{\xi}_i$	0	$\frac{1}{2}$	0	$\frac{1}{2}$	0	0	0

Table 2: Quantum numbers of the field components of the exact fermionic zero modes.

The radial functions are obtained by solving ordinary coupled differential equations. The equations for the lepton zero modes are

$$\hat{u}' + 3a\,\hat{u} = -m_1\varphi\,\hat{w} \tag{A.12a}$$

$$\hat{w}' = -m_1\varphi\,\hat{u} \tag{A.12b}$$

18

The prime denotes differentiation with respect to r. The functions $a = a(r)$ and $\varphi = \varphi(r)$ are defined in eqs. (A.1) and (A.2). The equations for the λ^{SS} zero modes are

$$\hat{f}' + 4a\hat{f} = -(\mu/\sqrt{2})\varphi\,\hat{g} \qquad (A.13a)$$

$$\hat{g}' + (1/r - 2a)\hat{g} + (a - 1/r)\hat{h}_1 = -\sqrt{2}\mu\varphi\hat{f} \qquad (A.13b)$$

$$\hat{p}' = (m/\sqrt{2})\varphi\,\hat{h}_1 \qquad (A.13c)$$

$$\hat{h}_1' + (3/r)\hat{h}_1 + 3(a - 1/r)\hat{g} = \sqrt{2}m\varphi\,\hat{p} \qquad (A.13d)$$

where

$$\hat{h}_1 = \hat{g} + 2r^2\hat{h}\,. \qquad (A.14)$$

The mass parameters μ, m and m_1 are defined in Sect. 2. Notice that the pairs $(\hat{f}, \hat{g})$ and $(\hat{p}, \hat{h}_1)$ diagonalize the mass operator at infinity.

The Born approximation amounts to neglecting the off-diagonal term on the r.h.s. of eq. (A.12a). One solves eq. (A.12b) with $\hat{u}$ given by the pure instanton expression. (Compare eq. (A.10a) and eq. (A.8)). The result is eq. (14). Similarly, solving eqs. (A.13b) and (A.13d) with $\hat{f}$ given by the pure instanton expression (see eq. (A.5)) and with $\hat{p} = 0$ gives rise to eq. (12).

As discussed in Sect. 3, the calculation of the leading log arising from the "lepton" zero mode eq. (13) requires a knowledge of the scale at which eq. (14) is no longer valid. The asymptotic behaviour of the wave function is a falling exponential

$$\hat{u} = \hat{w} = c_0 \left(\frac{m_1}{r^3}\right)^{\frac{1}{2}} e^{-m_1 r}\,. \qquad (A.15)$$

The transition from the power law behaviour given by eqs. (A.8) and (14) to the asymptotic behaviour eq. (A.15) occurs at the distance scale m_1^{-1}. This is a general property that can be derived as follows. Let us approximate the wave function by eqs. (A.8) and (14) for $r \leq r_0$, and by eq. (A.15) for $r \geq r_0$. We thus replace the smooth transition region by a sharp transition at $r = r_0$. Requiring that the two components of the wave function be continuous across the transition point gives us two equations for the two unknowns r_0 and c_0. The solution is $r_0 = O(m_1^{-1})$ and $c_0 = O(y)$. This information is sufficient to determine the leading log in eq. (13).

The physical cutoff of the integral in eq. (19) occurs at the same scale. This is derived by applying a similar analysis to the bosonic field equations. The same techniques can be used to obtain the qualitative structure of the transition region for the gaugino zero modes, but this information is not necessary for our calculations.

19

III. Approximate zero modes and the massive propagator

The last issue that we discuss is the approximate zero modes originating from the Higgsino and λ^{SC} zero modes, and their relation to the propagators of the massive Feynman rules. Going to a partial waves basis, let us denote by G_0 the massless propagator with the quantum numbers of the Higgsino and λ^{SC} zero modes, i.e. $K_1 = 0$ and $K_2 = \frac{1}{2}$. The zero modes themselves will be denoted by the generic name Ψ_0. The massless radial propagator G_0 obeys the differential equation

$$H_0 \, G_0(r', r) = r^{-3} \, \delta(r - r') - |\Psi_0\rangle \langle \Psi_0| \, . \tag{A.16}$$

Notice the second term on the r.h.s. of eq. (A.16) that projects out the zero modes. On the other hand, the massive propagator G with the same quantum numbers solves the equation

$$(H_0 + V) \, G(r', r) = r^{-3} \, \delta(r - r') \, . \tag{A.17}$$

Now there is a simple delta function on the r.h.s. of the equation, because there are no exact zero modes with the given quantum numbers in the presence of the Higgs field.

We now show that at short distances, the exact propagator G must have a "large" component which represents the approximate zero modes. This will justify the use of the massless Feynman rules for the Higgsino and λ^{SC} zero modes in Figs. 1 and 2. We first observe that the matrix element of the Higgs field

$$E_1 = \langle \Psi_0 | \, V \, | \Psi_0 \rangle \tag{A.18}$$

between the zero modes is small (Explicitly $E_1 = \epsilon_{kn} \, gv/\sqrt{2}$ where the indices k and n count the superconformal and Higgsino zero modes respectively). If the zero modes have turned into finite energy bound states Ψ with $E \sim E_1$, the large component would simply be $|\Psi\rangle \, E^{-1} \, \langle \Psi|$. Now, the support of the zero modes is inside a potential well of radius ρ, and so for $r \ll m^{-1}$ it should make no difference whether the zero modes have turned into true bound states or into resonances. Let us denote the first Born correction by

$$\Psi_1 = -G_0 V \Psi_0 \, . \tag{A.19}$$

One can check by direct substitution that for $r \ll m^{-1}$, the massive propagator G is related to the massless propagator G_0 by

$$G = G_0 + |\Psi_0 + \Psi_1\rangle \, E_1^{-1} \, \langle \Psi_0 + \Psi_1| + O(g) \, . \tag{A.20}$$

In the instanton's core, the r.h.s. of eq. (A.20) contains an $O(1/g)$ term which is an antisymmetric product of the original zero modes.

Within the massive Feynman rules, the first factor in eq. (8) is regarded as a part of fermionic determinant, i.e. as a part of the measure. Keeping track of the relation between the diagrams drawn using the massive and the massless Feynman rules, we find that the application of the massless Feynman rules to the Higgsino and λ^{SC} zero modes in Figs. 1 and 2 is justified.

Last we discuss the cancellation of logarithmic IR divergences related to the Higgsino and λ^{SC} zero modes. Such a logarithmic divergence can arise within the massless rules, if the two $\bar{\psi}(x)$ wave functions which are to be integrated over at the $\bar{\psi}\bar{\psi}\phi_0^*$ vertex behave like $1/x^2$ for $\rho \ll |x|$. As an example, the integration over that vertex is logarithmically divergent in each of the three diagrams shown in Fig. 5. But if we first sum the three integrands (still using the massless Feynman rules) the integration over the $\bar{\psi}\bar{\psi}\phi_0^*$ vertex becomes IR convergent. (As in Sect. 3, the integration over that vertex is done after the integration over the external point eq. (11). Notice also that the diagrams in Fig. 5 contain no logarithmic factors due to the $\bar{\xi}\bar{\xi}$ vertex. The propagator lines, which replace the classical fields in Fig. 1, lead to a $\bar{\xi}(x)$ wave function which is damped at least by an extra $1/x^2$).

In Fig. 5(a), the logarithmic divergence arises from the first Born correction to the λ^{SC} zero mode, which behaves like $\bar{\psi}(r) \sim 1/r^2$ for $r \gg \rho$. Fig. 5(b) is a mixed case. In Fig. 5(c), the logarithmic divergence arises from the partial wave of the $G_0 = \left\langle \psi \bar{\psi} \right\rangle_0$ propagator with the same total angular momenta as the Higgsino and λ^{SC} zero modes. For $r, r' \gg \rho$, the propagator $G_0(r', r)$ has a piece that behaves like $1/(r^2 r'^3)$. The $\bar{\psi}$ end of the propagator behaves like $1/r^2$. (This is most easily seen by writing the propagator in a Dirac spinor basis). The reason for this unusual behaviour is the projection on the (Higgsino) zero modes on the r.h.s. of eq. (A.16).

Notice that the product of a Higgsino zero mode $\psi(r')$ times the first Born correction $\bar{\psi}(r)$ to a λ^{SC} zero mode behaves like $1/(r^2 r'^3)$ too. An inspection of eq. (A.20) reveals that the massive radial propagator $G(r', r)$ contains the two sources of a $1/(r^2 r'^3)$ behaviour described above.

We will now show that the two $1/(r^2 r'^3)$ contributions on the r.h.s. of eq. (A.20) exactly cancel each other . The massive propagator $G(r', r)$ is a solution of eq. (A.17). In the intermediate region $m^{-1} \gg r, r' \gg \rho$, one can neglect *both* the gauge field and the Higgs field. The dominant term in the equation is the free massless Dirac operator. Every piece of the radial propagator $G(r', r)$ must therefore be the product of two homogeneous solutions of the free massless Dirac equation. For $r > r'$, the possible terms are $1/r^3$ and $1/(r r')^3$. Corrections to these terms are damped by inverse powers of r and/or r'. In particular, a $1/(r^2 r'^3)$ behaviour is inconsistent with eq. (A.17) for $r > r'$, and so it must cancel between the first and second terms on the r.h.s. of

eq. (A.20).

Within the massive Feynman rules, the three diagrams of the massless Feynman rules (Fig. 5) are contained in a single diagram (Fig. 6). In this diagram one should use massive propagators. The thick lines now correspond to various components of *exact* zero modes. Sub-graphs describing the mixing of the Higgsino and λ^{SC} zero modes are absent, as they are regarded as a part of the the fermionic determinant. All other effects of the approximate zero modes are now contained in the massive fermion propagators.

The cancellation of the $1/(r^2 \, r'^3)$ terms on the r.h.s. of eq. (A.20) implies that the massive diagram Fig. 6 makes no logarithmic contribution to $\langle \phi_0 \rangle$. We comment that, as a consequence of the absence of logarithmic terms, the sum of the three massless diagrams (Fig. 5) will be finite provided we amputate the external ϕ_0 leg. Following the general pattern discussed in the introduction, that sum will be equal to the corresponding amputated massive diagram up to higher order corrections.

As we have explained in Sect. 3, this cancellation occurs because subleading corrections to the wave function of an approximate zero mode cannot be disentangled from the continuous spectrum. This behaviour is natural if the zero mode has turned into a resonance. The new $\bar{\psi}$ component of the λ^{SC} zero mode is then responsible for its ultimate decay. In principle, there is also the possibility that the approximate zero mode has turned into a finite energy bound state. But since the energy of such a bound state is $O(m)$, it should behave like a resonance in the intermediate region $m^{-1} \gg r \gg \rho$. The $\bar{\psi}$ component of the λ^{SC} zero mode should then starts decaying outside of the potential barrier of radius ρ, but eventually it would remain trapped due to the mass term that changes the asymptotic value of the potential.

The massless diagrams shown in Fig. 5 involve the same m_0^*-dependent vertex as Fig. 1. There is a similar set of massless diagrams with the m_0^*-dependent vertex of Fig 2. Their sum is contained in the massive diagram shown in Fig. 7. (These massless diagrams can be retrieved from Fig. 7 in the same way that the massless diagrams of Fig. 5 are retrieved from Fig. 6). As before, the massive diagram Fig. 7 makes no logarithmic contribution to $\langle \phi_0 \rangle$. Finally, in Fig. 8 we show two massive diagrams that contain a closed loop. Their sum is UV finite, and neither diagram contains a logarithmic IR term.

References

[1] G. Veneziano and S. Yankielowicz, Phys. Lett. **B113** (1982) 321; T. Taylor, G. Veneziano and S. Yankielowicz, Nucl. Phys. **B218** (1983)493.

[2] E. Witten, Nucl. Phys. **B185** (1981) 513; Nucl. Phys. **B202** (1982) 253.

[3] I. Affleck, M. Dine and N. Seiberg, Nucl. Phys. **B241** (1984) 493.

[4] D. Amati, K. Konishi, Y. Meurice, G.C. Rossi and G. Veneziano, Phys. Rep. **162** (1988) 169 and references therein. G. Veneziano, Phys. Lett. **B124** (1983) 357.

[5] V. Novikov, M. Shifman, A. Vainshtein and V. Zakharov, Nucl. Phys. **B223** (1983) 445; Nucl. Phys. **B229** (1983) 381, 407; Nucl. Phys. **B260** (1985) 157.

[6] N. Seiberg, Phys. Rev. **D49** (1994) 6857. E. Witten, Jour. Math. Phys. **35** (1994) 5101. K. Intriligator, R.G. Leigh and N. Seiberg, Phys. Rev. **D50** (1994) 1092. K. Intriligator, and N. Seiberg, Nucl. Phys. **B431** (1994) 551. N. Seiberg and E. Witten, Nucl. Phys. **B426** (1994) 19; **431** (1994) 484.

[7] A. Casher and Y. Shamir, Phys. Rev. **D39** (1989) 514;

[8] A. Casher and Y. Shamir, Nucl. Phys. **B314** (1989) 390; Phys. Rev. **D40** (1989) 1356; Phys. Lett. **B274** (1992) 381.

[9] G. 't Hooft, Phys. Rev. **D14** (1976) 3432.

[10] Y. Frishman and S. Yankielowicz, Phys. Rev. **D19** (1979)540. I. Affleck, Nucl. Phys. **B191** (1981) 429.

Figure captions

1. One of the two leading log contributions to $\langle \phi_0 \rangle$. The diagrams in Fig. 1 up to Fig. 5 are drawn using the massless Feynman rules. The thick lines that emanate from the instanton (the shaded circle) represent fermionic zero modes. The dotted lines that end with a cross represent insertions of the classical Higgs field. The vertex marked with a thick cross is linear in m_0^*.

2. The other leading log contribution to $\langle \phi_0 \rangle$.

3. The ϕ_0 tadpole: the common lower part of Figs. 1 and 2.

4. In the calculation of $\langle \lambda\lambda \rangle$ this sub-graph replaces the ϕ_0 tadpole in Figs. 1 and 2.

5. Cancellation of logarithmic IR divergences related to the superconformal and Higgsino zero modes. In each diagram the integration over the $\bar{\psi}\bar{\psi}\phi_0^*$ vertex is logarithmically IR divergent. As shown in part III of the Appendix, the logarithmic IR divergences cancel among these diagrams before the ρ-integration.

6. This diagram, drawn using the massive Feynman rules, corresponds to the sum of the three massless diagrams in Fig. 5. It makes no logarithmic contribution to $\langle \phi_0 \rangle$.

7. Another massive diagram that makes no logarithmic contribution to $\langle \phi_0 \rangle$. This diagram contains the same m_0^*-dependent vertex as Fig. 2.

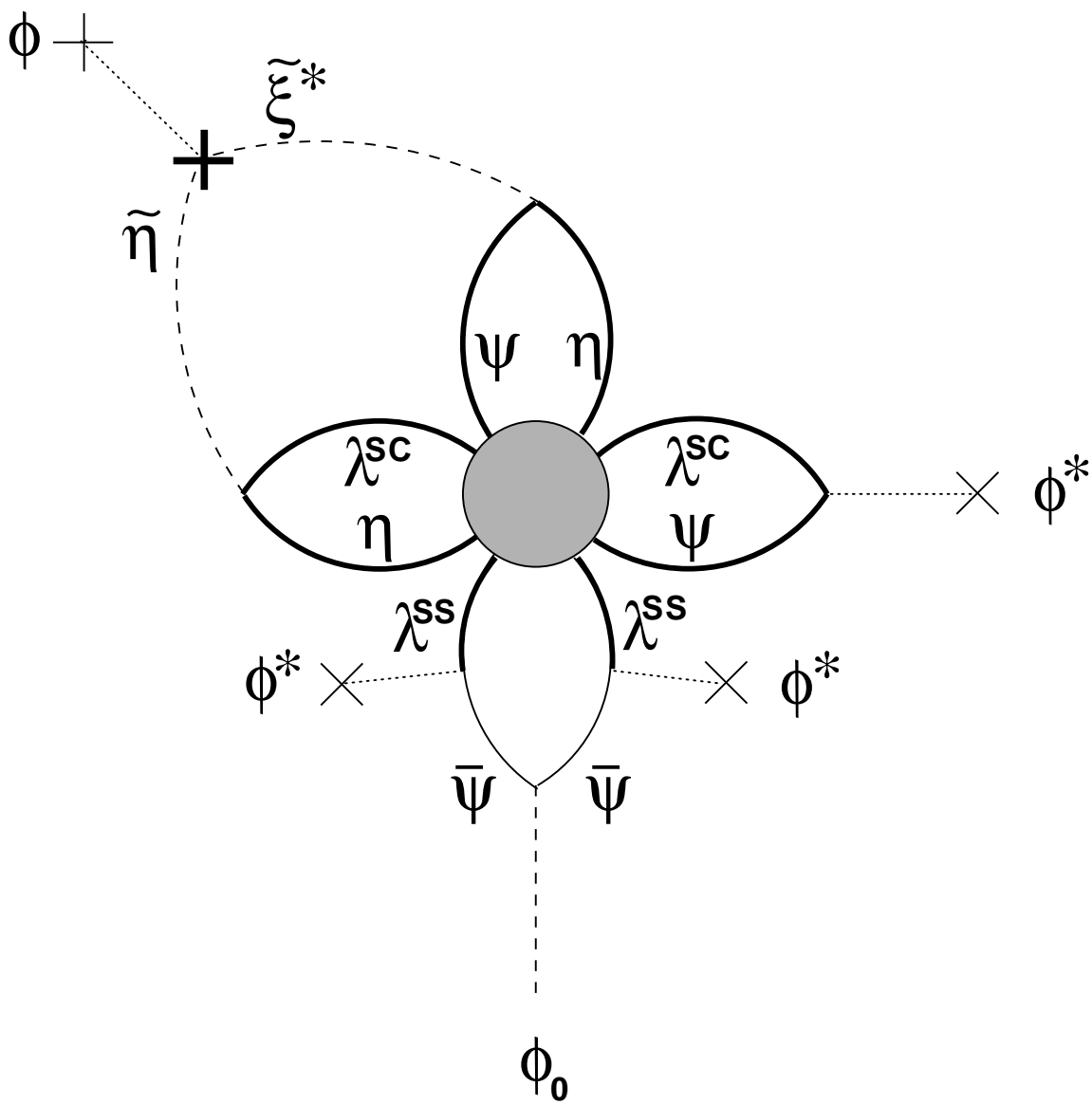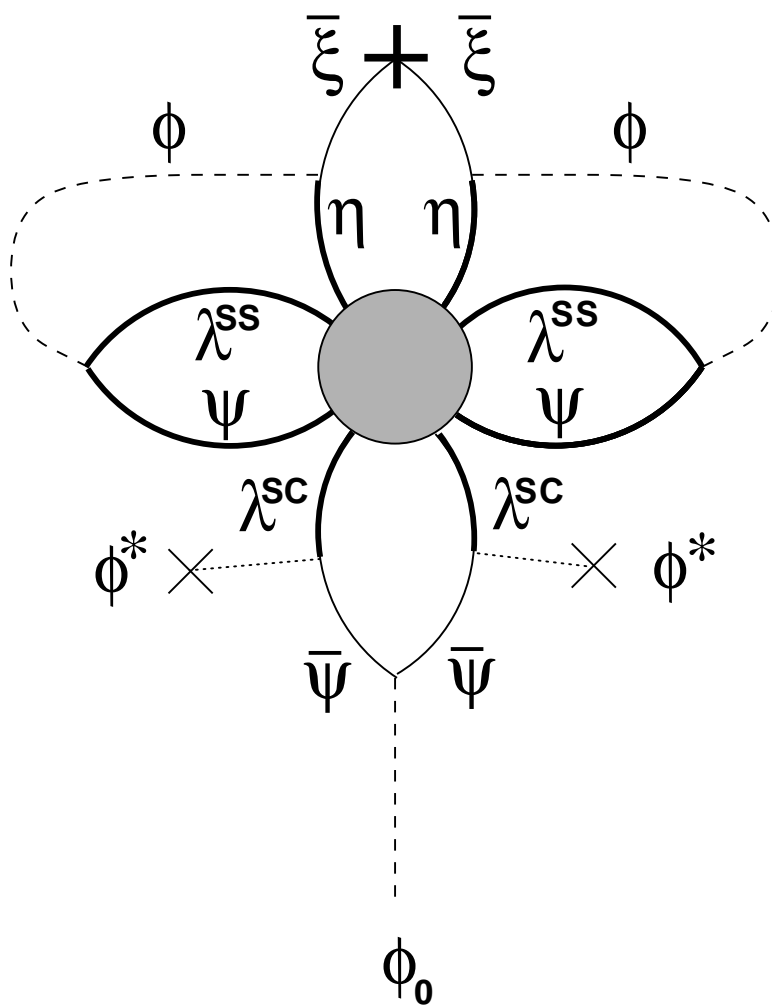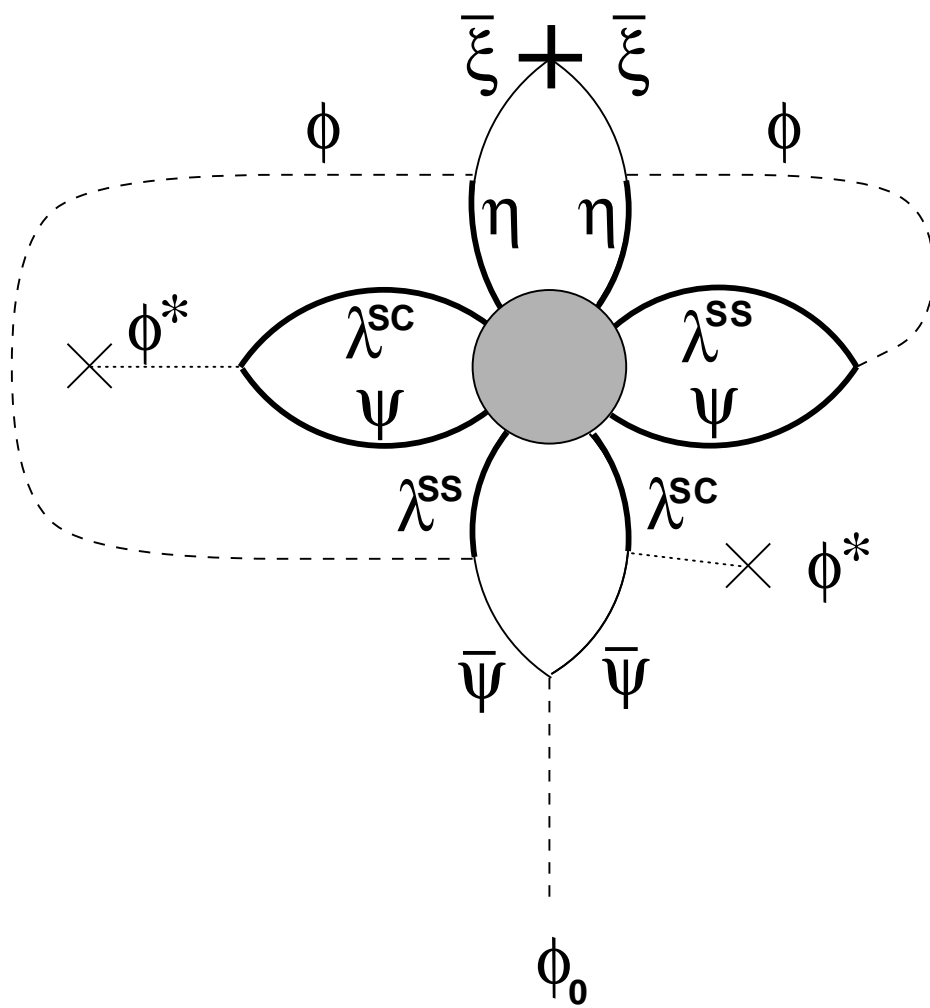8. Two massive diagrams containing a closed loop. Their sum is UV finite, and neither diagram contains a logarithmic IR term.
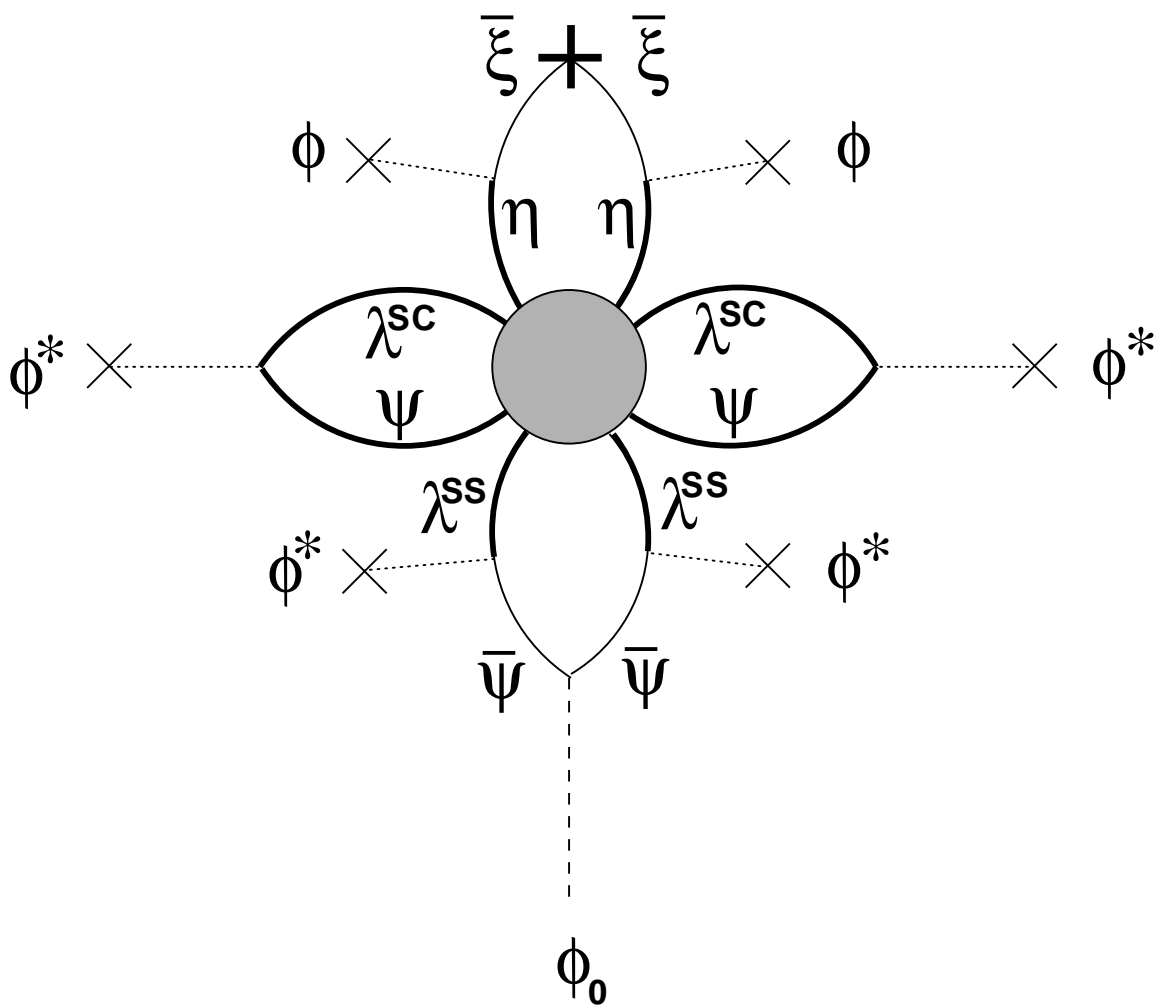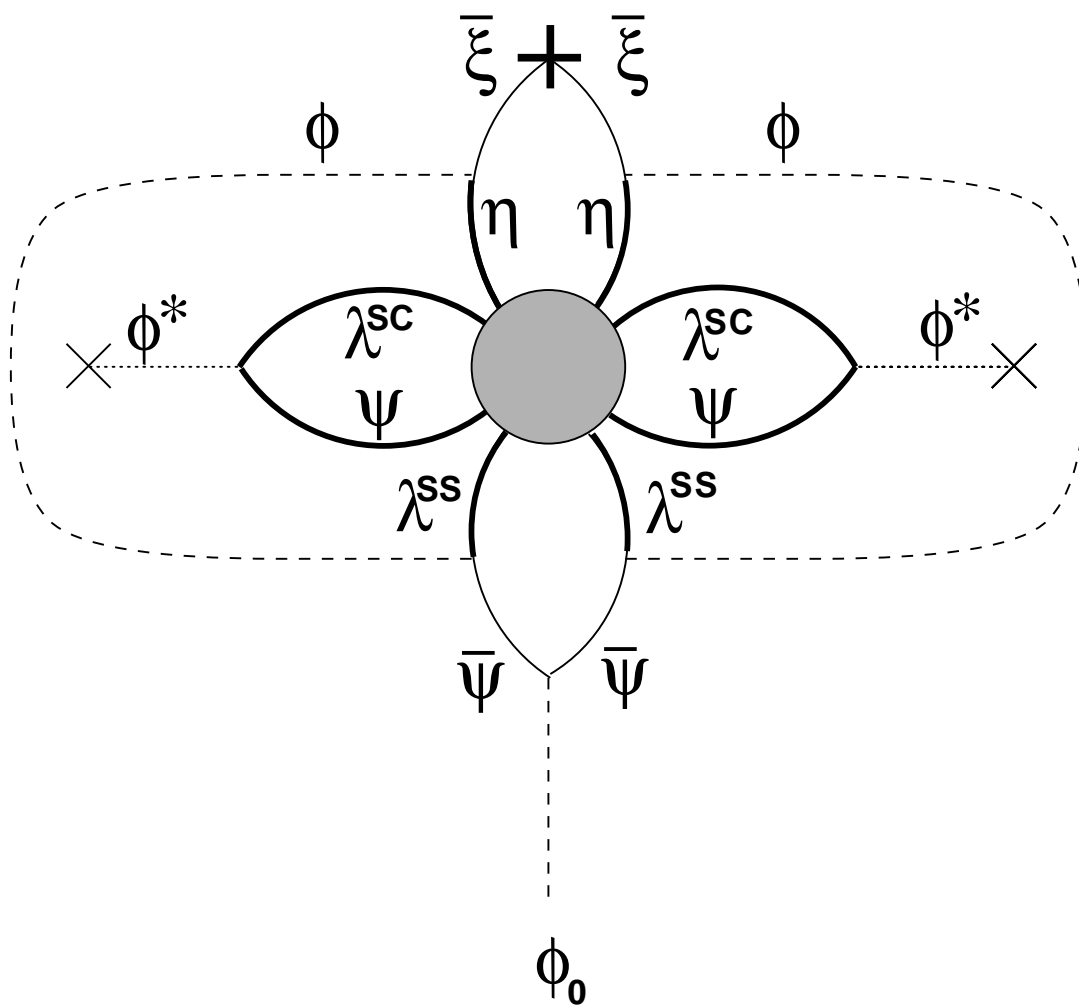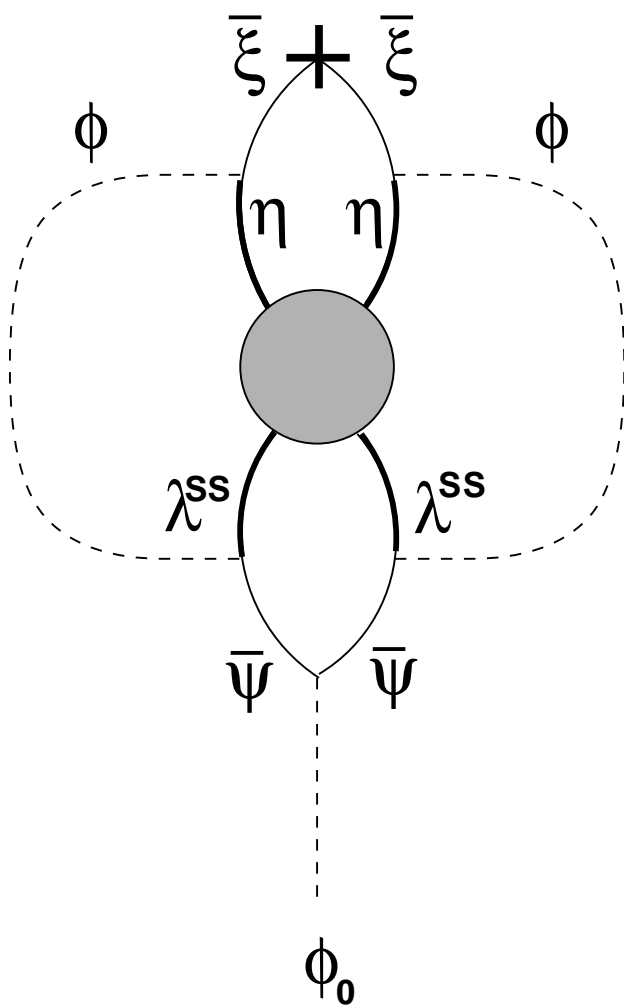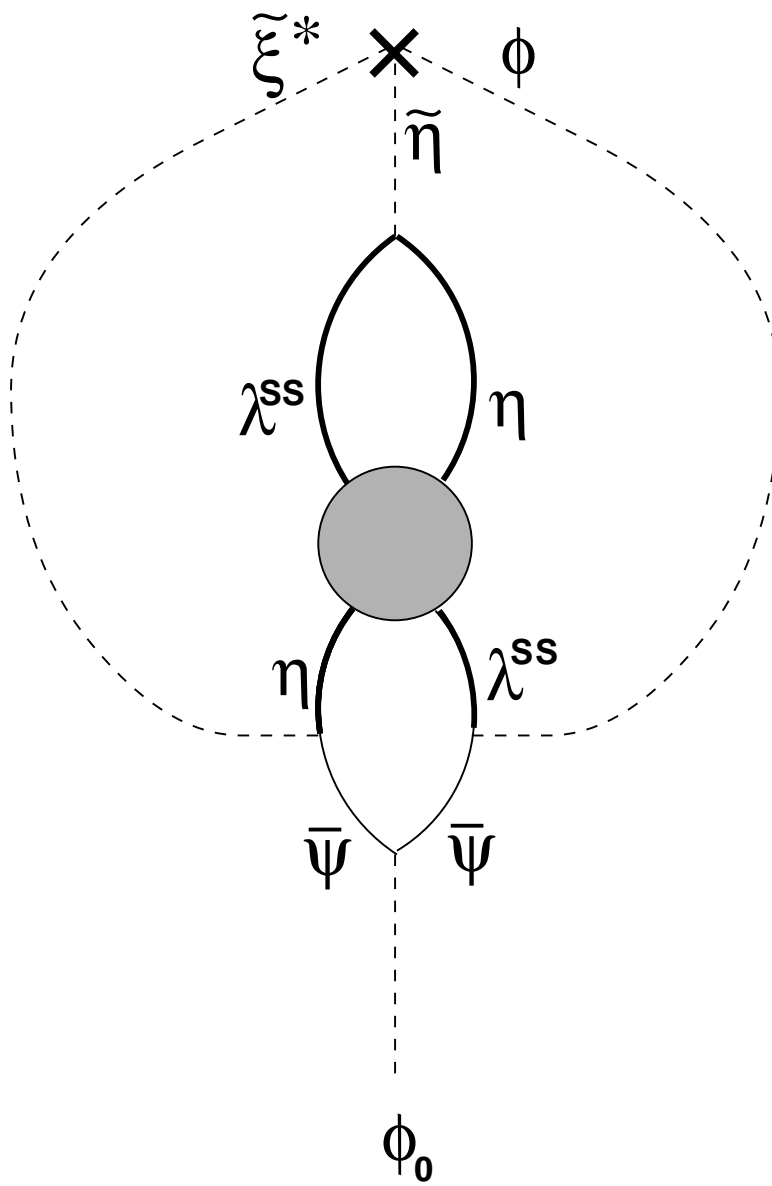
fig. 1

fig. 2

fig. 5(a)

fig. 5(b)

fig. 5(c)

fig. 6

fig. 7

fig. 8(a)

fig. 8(b)

λ^{ss} λ^{ss}

$\phi^* \times$ $\times \phi^*$

$\bar{\Psi}$ $\bar{\Psi}$

fig. 3

ϕ_0

fig. 4

λ^{ss} λ^{ss}